Solid Oxide Fuel Cell Material Structure Grading in the Direction Normal to the Electrode/Electrolyte Interface using COMSOL Multiphysics®

M. Andersson*, B. Sundén, Department of Energy Sciences, Lund University, Sweden

*Corresponding author: P.O. Box 118, 22100 Lund, Sweden, martin.andersson@energy.lth.se

Abstract: Fuel cells (FCs) are promising as an energy producing device, which at this stage of development will require extensive analysis and benefit from numerical modeling at different time- and length scales. COMSOL Multiphysics is used to describe an intermediate temperature solid oxide fuel cell (SOFC). Governing equations for heat, gas-phase species, electron, ion and momentum transport are implemented and coupled to kinetics describing electrochemical as well as internal reforming reactions. It is found, from the parameter study, that grading the electron tortuosity (decreased under the fuel and air channels), the electron conducting material fraction (increased under the fuel and air channels) and the pore tortuosity (decreased under the interconnect ribs), in the direction normal to the electrode/electrolyte interface increases the performance (average ion current density) slightly. On the other hand, is the performance slightly decreased from grading the porosity (increased under the interconnect ribs).

Keywords: Solid Oxide Fuel Cell, Design Optimisation, Structural Grading, 3D.

1. Introduction

FC science and technology cut across multiple disciplines, including (i) materials science, (ii) chemistry, (iii) electrochemistry, (iv) interfacial science, (v) heat transfer, (vi) mechanical engineering and (vii) catalysis [1]. The FC is not a new invention and its principle dates back to 1838 [2]. However, the FC technology is approaching the commercial phase, with an enormous future potential. The FC can be a key component in a future sustainable and efficient energy system. To reach commercialization the cell and system production costs must be decreased as well as the cell performance and the lifetime increased [3]. It is not an exaggeration to say that almost all problems have multiple scales in nature [4]. The particle size in solid oxide fuel cell (SOFC) functional materials is in the sub-micron scale, the three-phase boundary (TPB) structure, design and catalytic activity are in the nano- and mesoscales, compared to the cell and stack design which are in the macroscale. The morphology and properties of these scales are important for the performance of the FC. It means that the sciences at a mesoscopic scale are critical to the performance at a macroscopic scale. Strong coupling between the mentioned phenomena and scales makes multiphysics and multiscale SOFC modeling promising for optimizing the material structure and design, in order to increase the electrical efficiency and the cell lifetime [1,5].

A graded porosity can be used to maximize the three phase boundary (TPB) area-to-volume ratio (AV), since the TPB does not extend too far from the electrode/electrolyte interface. The high mechanical strength is maintained for the rest of the anode which is used as the cell support and for possible internal reforming reactions [6-7]. In practice, the porosity, pore- or particle radius graded electrodes can be manufactured by advanced ceramic techniques or by electrophoretic co-deposition [8]. An optimized pore structure decreases the gas-phase concentration differences between the fuel and/or air channel and the TPB, i.e., the concentration polarization decreases and also the Nernst potential increases from a higher concentration of fuel (at the anode TPB) and/or oxygen (at the cathode TPB), i.e., the current is increased. Also the ionic ohmic polarization can be decreased. A material structure with an increased effective thermal conduction lowers both the local temperature at the TPBs and the maximum cell temperature, which can increase the cell lifetime. Finally, it should be mentioned that a highly

optimized graded structure may contradict fuel flexibility.

The electrodes can be graded in several directions. Previous studies available in the open literature investigated graded structures through the electrodes in the direction normal to the main flow direction, and in terms of porosity and pore tortuosity, only [7]. It is expected that the novel approach, with grading in up-to three directions and the grading of additional structural parameters is an important step to enhance the scientific understanding concerning the fundamental transport phenomena within the electrodes (i.e., improving the cell performance) as well as to determine which parameters that is reasonable to grade. All efforts to decrease the different polarizations result in an increased current as well as electrical efficiency (if operating conditions are kept constant).

The aim of this paper is to investigate the impact from electrode material structural grading. The pore tortuosity, electron tortuosity, porosity and material composition volume fraction are graded in the parameter study in the z direction, i.e., the direction normal to electode/electrolyte interface.

2. Use of COMSOL Multiphysics

A model in three-dimensions is developed, in COMSOL Multiphysics version 4.3.2.189, to illustrate a planar intermediate temperature (IT) solid oxide fuel cell (SOFC). The transport equations are coupled to kinetics describing electrochemical and internal reforming reactions and are segregated in 5 different groups: *1.* velocity field, pressure distribution and pressure corrections, *2.* mass fraction distribution on the fuel side ($H_2/H_2O/CO/CO_2/CH_4$), *3.* ion and electron distribution, *4.* mass fraction distribution on the air side (O_2/N_2) and *5.* temperature distribution. The segregated solver is applied for 5 750 000 degrees of freedom and the solution tolerance is defined to 0.001 for each segregated group. Grid independence was achieved at 697 000 elements. The calculation time is around 24 hours on a single computer with 16 GB RAM and a CPU with 3.40 GHz. It should be noted that it is hard to give an exact value for the calculation time since the model is built in several steps, where each step start its calculation from the previous one.

The geometry is defined in Table 1, and a sketch of the investigated cell can be seen in Fig. 1. Note that Fig. 1 is not to scale.

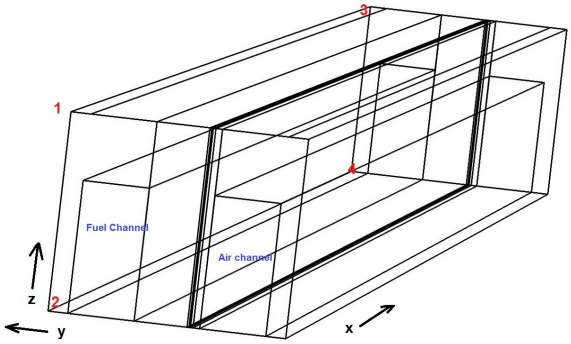

Figure 1. **Schematic figure of the SOFC model.**

Table 1: SOFC cell geometry

Cell Component	Direction	Thickness
Cell length	x	100 mm
Fuel & Air channel height	y	0.5 mm
Fuel & Air channel width	z	1 + 1 mm
Channel wall (rib) thickness	z	0.5 + 0.5 mm
Anode support layer thickness	y	400 μm
Anode active layer thickness	y	15 μm
Cathode support layer thickness	y	50 μm
Cathode active layer thickness	y	20 μm
Electrolyte thickness	y	10 μm
Interconnect thickness	y	150 +150 μm

2.1 Governing equations

Due to internal resistance and polarizations (overpotentials) the actual voltage (E) becomes less than the open-circuit voltage and can be expressed as [9-10]:

$$E = E^{OCV} - \eta_{act} - \eta_{ohm} \quad (1)$$

Here, η are the respective polarizations. The polarizations other than η_{ohm} are defined as:

$$\eta_a = \phi_s - \phi_l - E_{eq,a} \quad (2)$$

$$\eta_c = \phi_s - \phi_l - E_{eq,c} \quad (3)$$

where E_{eq} is the equilibrium voltage and ϕ the potential. The index c stands for the cathode, a for the anode, s for the electrode material (LSM or Ni) and l for the electrolyte material (YSZ).

The electromotive force (reversible open-circuit voltage, E^{OCV}) in eqn (1) is determined by the difference in the thermodynamic potentials of the electrode reactions. If the fuel is simplified to a hydrogen-steam mixture, it can be calculated by the Nernst equation [11-12]:

$$E^{OCV}_{H_2/O_2} = E^0_{H_2/O_2} - \frac{\mathrm{R}\cdot T}{2\cdot \mathrm{F}} \cdot \ln\left(\frac{p_{H_2O,TPB}}{p_{H_2,TPB}\sqrt{p_{O_2,TPB}}}\right) \quad (4)$$

$$E^0_{H_2/O_2} = 1.253 - 2.4516\cdot 10^{-4}\cdot T \quad (5)$$

where p_i is the partial pressure, at the TPB, in atm and E^0 the temperature dependent open-circuit voltage at standard pressure (1 atm).

The governing equations for the ion and electron transport are implemented according to eqns (6)-(7) (called "Secondary Current Distribution" in COMSOL):

$$i_l = \nabla \bullet \left(-\sigma_l \nabla \phi_l\right) \quad (6)$$

$$i_s = \nabla \bullet \left(-\sigma_s \nabla \phi_s\right) \quad (7)$$

where ϕ is the potential and σ the ion/electron conductivity and. The electronic conductivities in the anode ($\sigma_{s,a}$) and the cathode ($\sigma_{s,c}$), and ionic conductivity in the YSZ ($\sigma_{l,el}$) are calculated as described in [13]. The actual length that ions and electrons are transported in the electrodes increases because of the effects of the material compositions and their microscopic structures. This is accounted for by using the structure-dependent volume fractions/porosities and tortuosity factors [13].

Equation (8), named "Free and Porous Media Flow" in COMSOL, is introduced and solved for the momentum transport (gas flow) in the fuel and air channels as well as in the porous materials, simultaneously [14-15], i.e., the interface conditions between the porous electrodes and the gas channels do not need to be defined.

$$\left(\frac{\mu}{\kappa} + \rho\cdot\nabla\bullet\vec{\mathrm{u}}\right)\cdot\vec{\mathrm{u}} - \nabla\left[-p + \frac{1}{\varepsilon}\left\{\Psi - \left(\frac{-2}{3}\cdot\mu\right)(\nabla\bullet\vec{\mathrm{u}})\right\}\right] = \mathbf{F} \quad (8)$$

Here $\mathbf{F}$ is the volume force vector, p the pressure, κ the permeability of the porous medium ($1.76\cdot10^{-11}$ m^2 is applied for all porous material in our model), $\vec{\mathrm{u}}$ the velocity vector, Ψ the viscous stress tensor. The viscosity (μ) and density (ρ) for the participating gas mixtures are dependent on local temperature and mole fractions.

Equation (9), called "Transport of Concentrated Species" in COMSOL, is used to describe the gas-phase species transport phenomena for each component inside the cell [15] and solved for the fuel and air channels as well as for the electrodes simultaneously, i.e., no interface condition need to be defined.

$$\nabla\left(-\rho\cdot w_i\sum_{}^{n} D_{eff,ij}\cdot\nabla x_j + \left(x_j - w_j\right)\frac{\nabla p}{p}\bullet\vec{\mathrm{u}}\right) + \rho\cdot\vec{\mathrm{u}}\cdot\nabla w_j = S_i \quad (9)$$

where x is the mole fraction, w the mass fraction and S_i the (mass) source term due to electrochemical reactions.

The overall governing equation for the heat transport (named "Heat Transfer in Fluid" in COMSOL) is defined in eqn (10):

$$\rho_g\cdot c_{p,g}\cdot\vec{\mathrm{u}}\cdot\nabla T = \nabla\bullet\left(k_{eff}\nabla T\right) + Q_h \quad (10)$$

Here Q_h is the heat generation or consumption, k_{eff} the effective thermal conductivity, T the temperature and c_p the gas-phase specific heat. The Q_h is based on heat generation by the electrochemical reactions, ohmic as well as activation polarizations and consumption by the internal reforming reactions:

$$Q_h = i\cdot\left(\frac{T\cdot\Delta S_r}{n_e\cdot\mathrm{F}} + \eta_{act}\right) + \sum\frac{i^2}{\sigma} + \sum\left(r_{ref}\cdot\Delta H_{ref}\right) \quad (11)$$

where ΔS_r is entropy change of the reaction, r_{ref} the reforming reaction rates (in mol/m^{3}s) and ΔH_{ref} the enthalpy change of the reforming reactions.

2.2 Boundary conditions

The gas inlet velocities are defined by laminar flow profiles. The inlet fuel velocity is adjusted to reach fuel utilization of 80 % for the standard case. The same amount of fuel is supplied for each case in the parameter study. The inlet air velocity is adjusted to limit the average temperature difference between the inlets and outlets to 100 K for the standard case, and is kept constant in the parameter study. At the outlets the pressure (1 atm) is fixed. The fuel inlet fractions are defined as 30 % pre-reformed natural gas (as defined by International Energy Agency (IEA) [1]), the air inlet is defined as air, including oxygen and nitrogen, and the outlets are defined as convective fluxes. The inlet gas temperature is defined by the operating temperature (1000 K, for all cases) and the outlet is defined as a convective flux. The boundaries at the top, bottom and centre of the cell walls are defined as symmetry conditions, because it is assumed that the cell is surrounded by other ones with the identical temperature distribution. The potential at the anode current collector is set to zero and the potential at the cathode current collector is set as the cell operating voltage (0.7 V). All other boundaries and interfaces are electrically insulated.

3. Parameter study

A standard case is defined based on the authors previous modeling work [16]. Material grading are defined in the z-direction (see Fig. 1) considering:

1. The pore tortuosity, is multiplied with a factor varying between 0.5 and 1.5, with a decreased pore tortuosity at positions under the interconnect ribs
2. The electron tortuosity, is multiplied with a factor varying between 0.5 and 1.5, with a decreased electron tortuosity at positions under the air and fuel channels
3. The porosity, is varied ± 0.10 compared to the average value, with an increased porosity under the interconnect ribs.
4. The material composition volume fraction, is varied ± 0.10 compared to the average value, with an increased electron conducting material fraction under the fuel and air channels and consequently an increased ion conducting material fraction under the interconnect ribs.

It should be mentioned that the average of the graded parameter is kept constant in all investigations and only one parameter is varied at the same time. Notice, that the operating parameters are kept the same for all cases. Note that a combination of the different graded material structures are outside the scope of this study.

4. Result and Discussion

The temperature profile in 3D is presented in Fig. 2. The air inlet velocity is adjusted to reach an average temperature difference between the inlets and outlets to 100 K for the standard case.

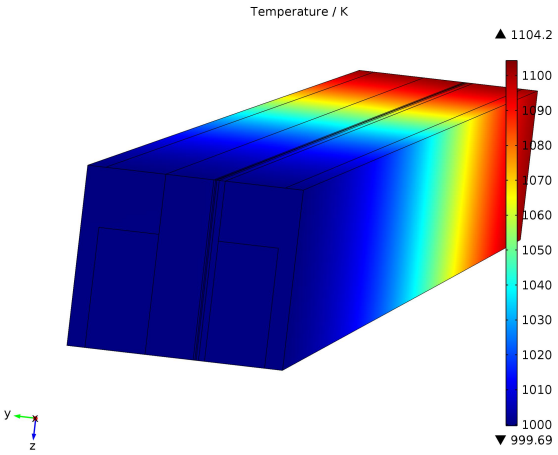

Figure 2. Temperature distribution in 3D for the standard case.

The oxygen distribution (in terms of mole fraction) for the standard case is presented in Fig. 3. It is clear that the mole fraction gradient in the direction normal to the cathode/electrolyte interface at positions under the interconnect ribs becomes significant, i.e., the electrochemical reactions are limited from the amount of available oxygen at these specific positions.

The ion current density at the cathode/electrolyte interface is shown in Fig. 4

for the standard case. The current density increases along the main flow direction (x*-direction) as the temperature increases. The ion current density in the direction normal to the main flow direction is highest at positions where the oxygen fraction is high as well as the electron transport path is short. The average ion current density is 1597 A/m^2.

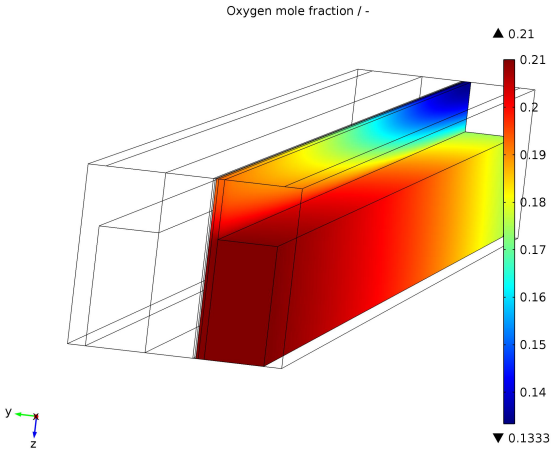

Figure 3. Oxygen mole fraction in 3D for the standard case.

The OCV at the cathode/electrolyte interface is presented in Fig. 5 for the standard case. The OCV is mainly influenced by the temperature, i.e., the OCV decreases as the temperature increases along the main flow direction.

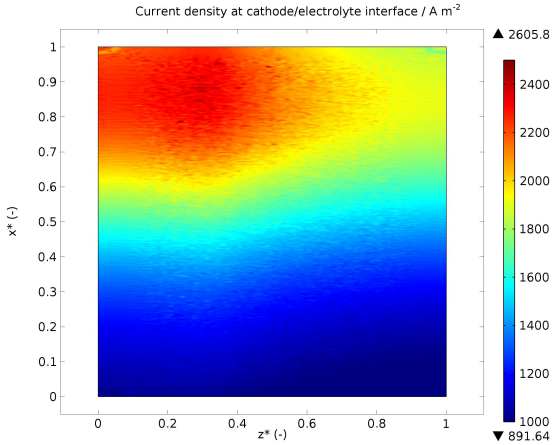

Figure 4. Ion current density at the cathode/electrolyte interface for the standard case.

The electron current densities in the direction normal to the main flow direction are presented

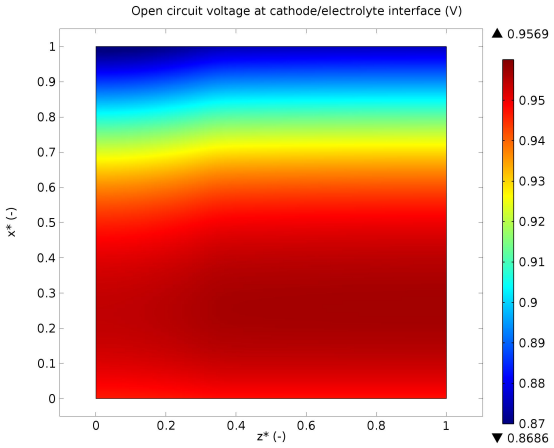

Figure 5. OCV for the standard case.

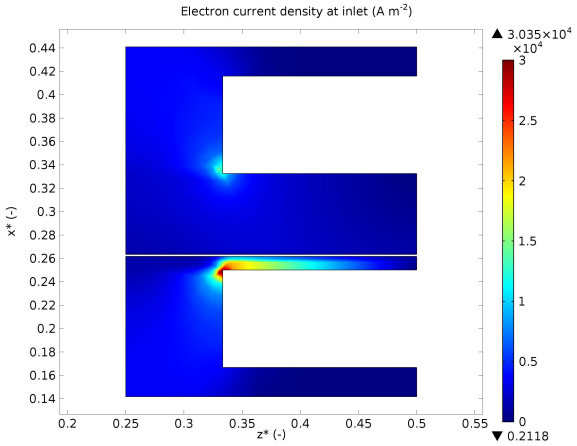

Figure 6. Electron current density at the inlet for the standard case.

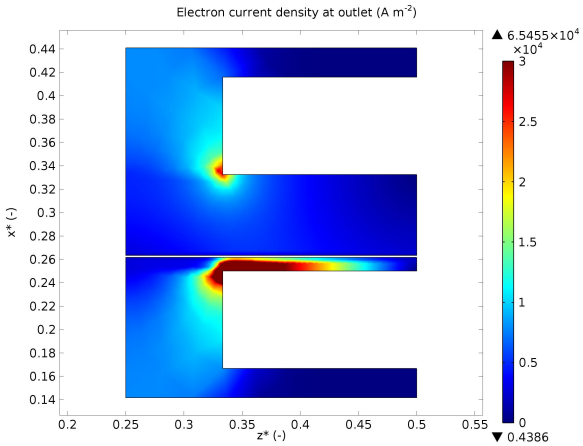

Figure 7. Electron current density at the outlet for the standard case.

in Figs 6-7 for the inlet and for the outlet, respectively, for the standard case. It is clear that

the maximum electron current density is more than 20 times higher than the maximum ion current density. It is also shown that the maximum value on the fuel side is around 40 % of the maximum value on the air side. The (electron and ion) current density is higher at the outlet compared to the inlet mainly due to the increased temperature.

The reaction rate for the MSR is presented in Fig. 8 and for WGSR in Fig. 9. The MSR rate is highest close the fuel inlet and decreases along the main flow direction as the concentration of methane decreases. The WGSR rate is also high close to the fuel inlet, due to conditions far from equilibrium, and continues to produce more hydrogen as water is produced throughout the anode.

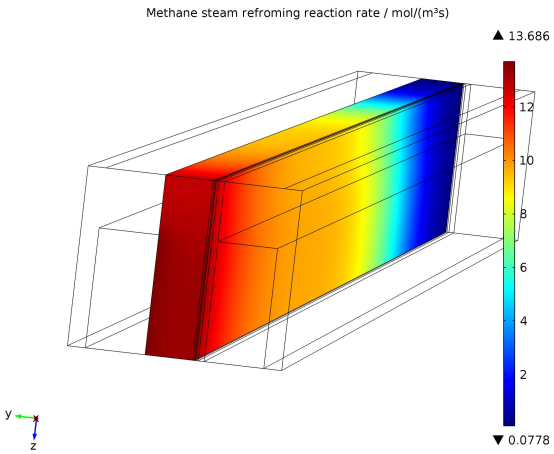

Figure 8. MSR rate within the anode for the standard case.

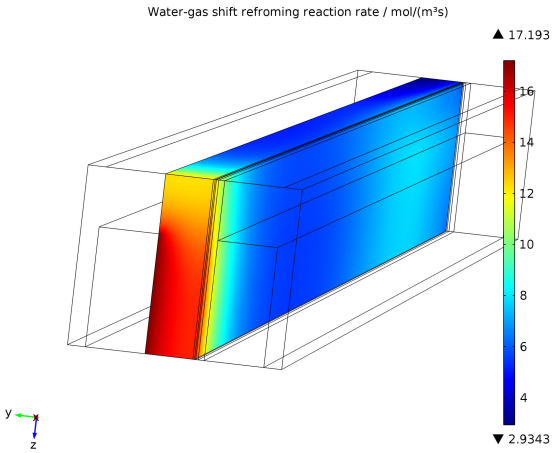

Figure 9. WGSR rate in the anode for the standard case.

The electron tortuosity is graded with a decreased electron tortuosity at positions under the fuel and air channels and consequently an increased electron tortuosity at positions under the interconnect ribs. The average electron tortuosity is kept constant compared to the standard case to be able to investigate the impact from the graded electron tortuosity only. The maximum current density (Fig. 10) increases and the minimum oxygen mole fraction (Fig. 11) decreases, which shows that the performance is improved. The average current density increases with 0.3 % compared to the standard case.

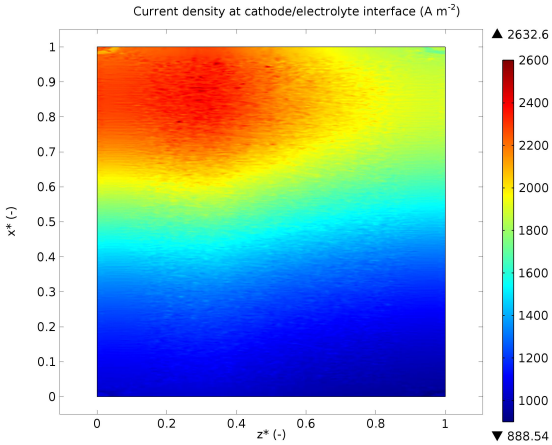

Figure 10. Ion current density for the case with graded electron tortuosity.

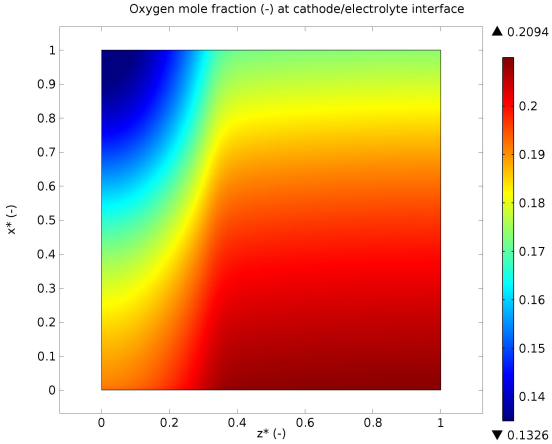

Figure 11. Oxygen mole fraction for the case with graded electron tortuosity.

The electron conducting material and ion conducting material volume fractions are graded (keeping the porosity constant). The electron conducting material volume fraction is increased

at positions under the fuel and air channels and the ion conducting material volume fraction is consequently increased at positions under the interconnect rips, keeping the average volume fractions constant (compared to the standard case). The performance is increased and the average current density increases with 0.5 % (Fig. 12) compared to the standard case, and also the oxygen consumption (Fig. 13) increases.

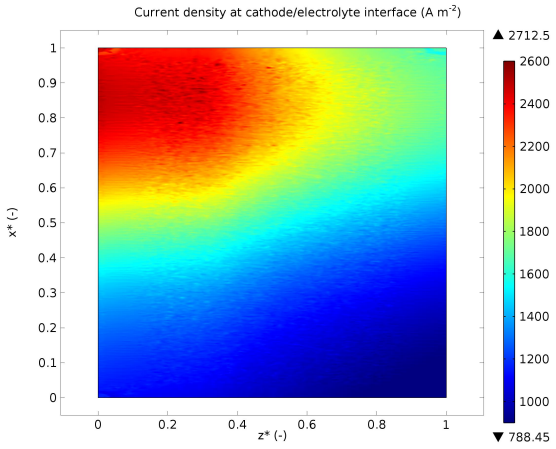

Figure 12. Ion current density for the case with graded electron/ion conducting material volume fractions.

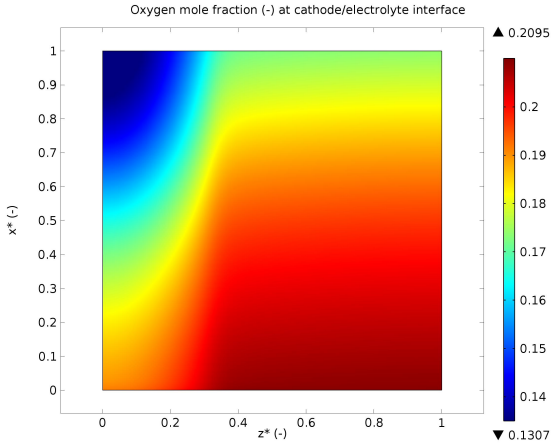

Figure 13. Oxygen mole fraction for the case with graded electron/ion conducting material volume fractions.

The porosity is graded with an increased porosity at positions under the interconnect ribs and a decreased porosity at positions under the fuel and are channels. The average current density decreases with 0.4 % (Fig. 14) compared to the standard case. The increased porosity under the interconnect ribs makes it easier for the oxygen molecules to be transported there, i.e., the minimum oxygen mole fraction increases which increases the OCV at these specific positions. The decreased current density can be explained from increased polarization losses, especially the increased ion resistance at positions with an increased porosity, i.e., a decreased ion conducting material volume fraction.

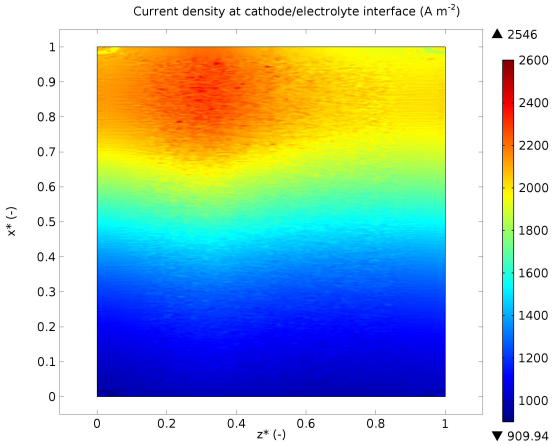

Figure 14. Ion current density for the case with graded porosity.

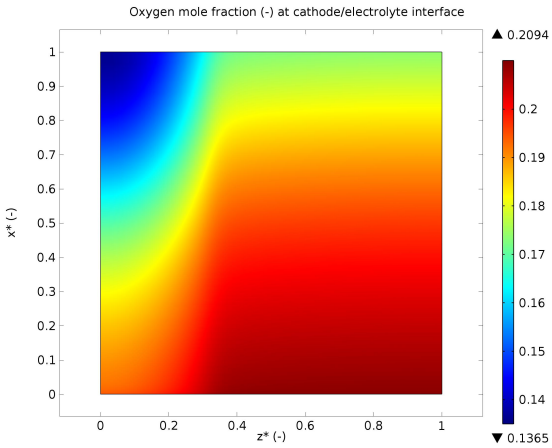

Figure 15. Oxygen mole fraction for the case with graded porosity.

The pore tortuosity is graded with a decreased pore tortuosity at positions under the interconnect ribs and an increased pore tortuosity at positions under fuel and air channels, compared to the standard case. The average

current density (Fig. 16) increases with 0.6 % compared to the standard case. The minimum oxygen mole fraction (Fig. 17) is significantly increased due to decreased tortuosity at the positions under the interconnect ribs, which increases the OCV.

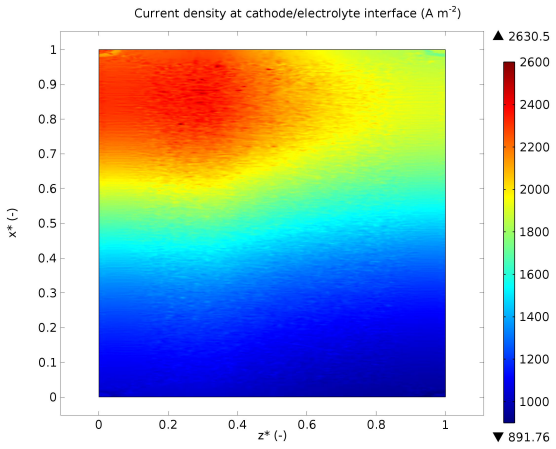

Figure 16. Ion current density for the case with graded pore tortuosity.

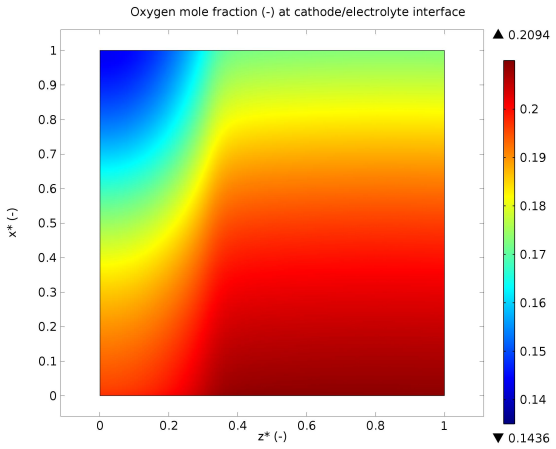

Figure 17. Oxygen mole fraction for the case with graded pore tortuosity.

5. Conclusions

COMSOL Multiphysics is used to describe an intermediate temperature SOFC. Governing equations for heat, gas-phase species, electron, ion and momentum transport are implemented and coupled to kinetics describing electrochemical as well as internal reforming reactions. A parameter study is performed focusing on grading the electrode material structure in terms of pore tortuosity, electron tortuosity, porosity and material composition volume fraction. It is found that grading the electron tortuosity (decreased under the fuel and air channels), the electron conducting material fraction (increased under the fuel and air channels) and the pore tortuosity (decreased under the interconnect ribs), in the direction normal to the electrode/electrolyte interface increases the performance (average ion current density) slightly. A further increased performance is expected if also the operating parameters are optimised to the graded material structure. The porosity is graded (increased under the interconnect ribs), in the direction normal to the electrode/electrolyte interface, to enhance the oxygen transport at positions under the interconnect ribs. The gas-phase oxygen transport resistance is decreased at these positions, however, the average ion current density is slightly decreased.

6. References

1. M. Andersson, *Solid Oxide Fuel Cell Modeling at the Cell Scale*, Doctoral dissertation, ISBN 9789174731804, Lund University (2011)
2. C.F. Schönbein Further Experiments on the Current Electricity Excited by Chemical Tendencies, Independent of Ordinary Chemical Action, *The London and Edinburgh Phil. M. and J. Sci.*, **12**, 311-317 (1838)
3. A. J. Jacobson, Materials for Solid Oxide Fuel Cells, *Chem. Mater.*, **22**, 660-674 (2010)
4. Y.-L. He, W.-Q. Tao, Multiscale simulations of heat transfer and fluid flow problems, *ASME J. Heat Transfer*, **134**, 031018 (2012)
5. M. Peksen, R. Peters, L. Blum, D. Stolten, Numerical modeling and experimental validation of a planar type pre-reformer in SOFC technology, *Int. J. Hydrogen Energy*, **34**, 6425-6436 (2009)
6. M. Andersson, J. Yuan, B. Sundén, Grading the amount of electrochemical active sites along the main flow direction of an SOFC, *J. Electrochemical Soc*, **160**, F1-F12 (2013)
7. L. Liu, R. Flesner, G.-Y. Kim, A. Chandra, Modeling of Solid Oxide Fuel Cells with Particle Size and Porosity Grading in Anode Electrode, *Fuel Cells*, **12**, 97-108 (2012)
8. Z. Wang, N. Zhang, J. Qiao, K. Sun, P. Xu, Improved SOFC performance with continuously

graded anode functional layer, *Electrochemistry Com.*, **11**, 1120-1123 (2009)
9. Y. Patcharavorachot, A. Arpornwichanop, A. Chuachuebsuk, Electrochemical Study of a Planar Solid Oxide Fuel Cell: Role of Support Structures, *Journal of Power Sources*, **177**, 254-261 (2008)
10. K. Oulmi, B. Zitouni, H.B. Moussa, H. Abdenebi, G.M. Andreadis, Total Polarization Effect on the Location of Maximum Temperature Value in Planar SOFC, *International Journal of Hydrogen Energy*, **36**, 4236-4243 (2011)
11. Fuel Cell Handbook (7th edition), U.S. DoE, Morgantown, West Virginia (2004)
12. W. Winkler, P. Nehter, Thermodynamics of Fuel Cells, *Fuel Cells and Hydrogen Energy*, **1**, 15-50 (2008)
13. M. Andersson, J. Yuan, B. Sundén, SOFC Modeling Considering Hydrogen and Carbon Monoxide as Electrochemical Reactants, *Journal of Power Sources*, **232**, 42-54 (2013)
14. M. le Bars, M.G. Worster, Interfacial Conditions Between a Pure Fluid and a Porous Medium, Implications for Binary Alloy Solidification, *Journal of Fluid Mechanics*, **550**, 149-173 (2006)
15. *COMSOL Multiphysics version 4.3 User Guide,* Stockholm, Sweden (2012)
16. M. Andersson, H. Nakajima, T. Kitahara, A. Shimizu, T. Koshiyama, H. Paradis, J. Yuan B. Sundén, Comparison of Humidified Hydrogen and Partly Pre-Reformed Natural Gas as Fuel for Solid Oxide Fuel Cells applying Computational Fluid Dynamics, Accepted for publication in *Int. J Heat and Mass Transfer* (2014)

7. Acknowledgements

The financial support from the Swedish Research Council (VR-621-2010-4581) and the European Research Council (ERC-226238-MMFCs) is gratefully acknowledged.